5614 *Inorg. Chem.* **2009**, *48*, 5614–5616
DOI: 10.1021/ic900697b

Inorganic Chemistry
Communication

Monodisperse F-Substituted Hydroxyapatite Single-Crystal Nanotubes with Amphiphilic Surface Properties

Junfeng Hui,[‡] Guolei Xiang,[†] Xiangxing Xu,[†] Jing Zhuang,[†] and Xun Wang*,[†]

[†]*Department of Chemistry, Tsinghua University, Beijing 100084, People's Republic of China, and* [‡]*R&D Center of Biomaterial and Fermentation Engineering, Shaanxi Key Laboratory of Degradable Biomedical Materials, Department of Chemical Engnineering, Northwest University, Xian 710069, People's Republic of China*

Received April 8, 2009

Uniform F-substituted HAp nanotubes with different aspect ratios and surface properties have been successfully prepared via a hydrothermal synthetic route. A small amount of 3% F doping into HAp can lead to the formation of nanotubes. This study will provide not only novel building blocks for the construction of artificial bones or other composites with novel mechanical properties but also a new strategy for the controlled growth of inorganic nanotubes.

Hydroxyapatite (HAp) and their F-substituted counterparts are the main inorganic components in both bones and teeth.[1] It is interesting that HAp's are in the form of short and long nanorods in bones and teeth, respectively. Undoubtedly, the unique mechanical properties of 1-D nanorods have endowed the bones and teeth with an excellent combination of ductility and hardness.[2,3] Up to now, uniform HAp nanorods with different aspect ratios and surface properties have been obtained via hydrothermal and microemulsion-based methods, etc., which provide novel building blocks for the construction of artificial bones.[4−8] It is well-known that single-crystal nanotube structures have shown even better mechanical properties over nanorod structures.[9−13] So, it would be quite interesting and promising if HAp or F-substituted HAp could be prepared as nanotube structures. However, because of the lack of synthetic strategies, there have been no reports on the controlled growth of single-crystal HAp nanotubes. In this Communication, monodisperse F-substituted HAp nanotubes with different aspect ratios have been obtained via a hydrothermal-based synthetic method. It is worth noting that a small amount of doping of ~3% F^- into the HAp nanorods can lead to the formation of single-crystal nanotubes.

The surface properties of monodisperse nanocrystals are usually the key for their application in different fields.[14−16] Despite the success in achieving hydrophilic[15] or hydrophobic[16] surface properties, up to now it is still a puzzle to obtain nanocrystals with amphiphilic surface properties. A recent study by Smith and Nie showed the possibility of achieving universal solubility in nanocrystals by controlling the surface structures of the ligands.[14] However, just like what the authors have mentioned, the change in the surface structures is not reversible, which means that the as-obtained nanocrystals are not inherently amphiphilic. Herein we report that the combination of poly(ethylene glycol) (PEG) with oleic acid will endow the HAp single-crystal nanotubes with universal solubility in both polar and nonpolar solvents-including water, ethanol, cyclohexane, and chloroform. The amphiphilic surface properties of these monodisperse F-HAp nanotubes will ensure better interface compatibility in organic−inorganic composites and thus satisfy the demands for the construction of high-quality artificial bones and other composite materials.[17,18]

The final products were first characterized with transmission electron microscopy (TEM) and high-resolution TEM (HRTEM). It was found that without doping uniform HAp nanorods could be obtained, just as described previously.[7,8] However, a small amount of doping of 3% F^- into the HAp nanorods could lead to the formation of uniform nanotubes. As shown in the Figure 1a, at a temperature of 100 °C, 1-D

---

*Corresponding author. E-mail: wangxun@mail.tsinghua.edu.cn.

(1) Vallet-Regí, M.; González-Calbet, J. M. *Prog. Solid State Chem.* **2004**, *32*, 1.
(2) Tiselius, A.; Hjerten, S.; Levin, O. *Arch. Biochem. Biophys.* **1956**, *65*, 132.
(3) Yoshimura, M.; Suda, H.; Okamoto, K.; Ioku, K. *J. Mater. Sci.* **1994**, *29*, 3299.
(4) Antonietti, M.; Breulmann, M.; Goltner, C.; Colfen, H.; Wong, K.; Walsh, D.; Mann, S. *Chem.—Eur. J.* **1998**, *4*, 2493.
(5) Hartgerink, J. D.; Beniash, E.; Stupp, S. I. *Science* **2001**, *294*, 1684.
(6) Sadasivan, S.; Khushalani, D.; Mann, S. *Chem. Mater.* **2005**, *17*, 2765.
(7) Wang, X.; Zhuang, J.; Peng, Q.; Li, Y. D. *Nature* **2005**, *437*, 121.
(8) Wang, X.; Zhuang, J.; Peng, Q.; Li, Y. D. *Adv. Mater.* **2006**, *18*, 2031.
(9) Poncharal, P.; Wang, Z. L.; Ugarte, D.; de Heer, W. A. *Science* **1999**, *283*, 1513.
(10) Wong, W. W.; Sheehan, P. E.; Lieber, C. M. *Science* **1997**, *277*, 1971.
(11) Dai, H. J. *Acc. Chem. Res.* **2002**, *35*, 1035.
(12) Goldberger, J.; He, R. R.; Zhang, Y. F.; Lee, S. W.; Yan, H. Q.; Choi, H. J.; Yang, P. D. *Nature* **2003**, *422*, 599.
(13) Goldberger, J.; Fan, R.; Yang, P. D. *Acc. Chem. Res.* **2006**, *39*, 239.
(14) Smith, A. M.; Nie, S. M. *Angew. Chem., Int. Ed.* **2008**, *47*, 9916.
(15) Zhang, T. R.; Ge, J. P.; Hu, Y. P.; Yin, Y. D. *Nano Lett.* **2007**, *7*, 3203.
(16) Wang, X.; Peng, Q.; Li, Y. D. *Acc. Chem. Res.* **2007**, *40*, 635.
(17) Wang, C. C.; Hsu, C. Y.; Hsieh, M. C.; Yang, S. P.; Su, F. C.; Lee, T. M. *Nanotechnology* **2008**, *19*, 335709.
(18) Fathi, M. H.; Hanifi, A.; Mortazavi, V. *J. Mater. Process. Technol.* **2008**, *202*, 536.

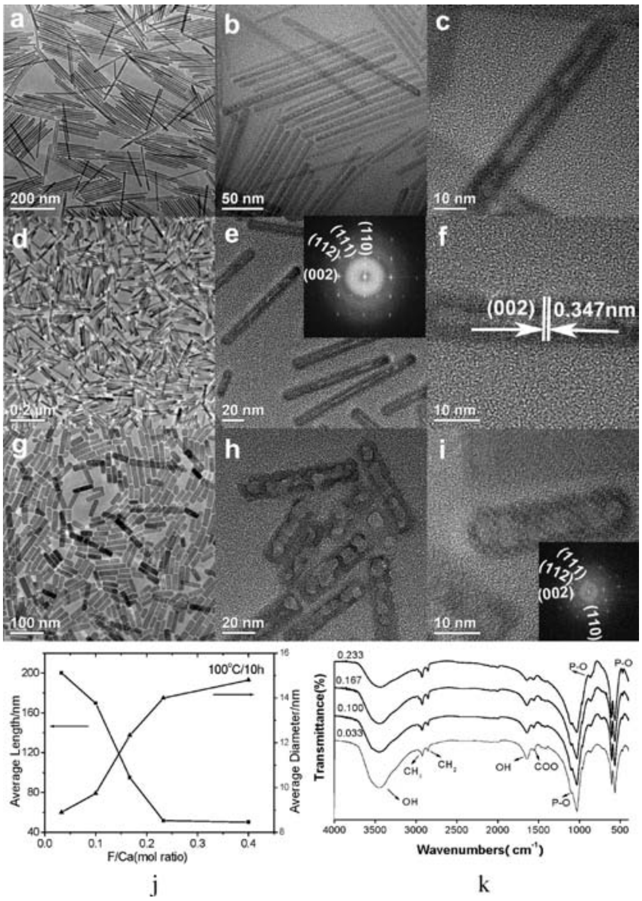

Figure 1. (a−i) Representative TEM and HRTEM images of F-HAp nanotubes with different doping levels: a−c, F/Ca = 0.033, 100 °C; d−f, F/Ca = 0.05, 100 °C; g−i, F/Ca = 0.25, 100 °C. (j) Variance of the lengths and diameters of nanotubes with differences in the F/Ca ratio. (k) IR spectra taken from F-HAp nanotubes with different doping levels.

nanorods with diameters of ~10 nm and lengths of ~200 nm can be obtained. All of the structures have nearly the same diameters and lengths, showing the effectiveness of this method in confining the sizes and dimensions of HAp. All of the structures are well-dispersed on the TEM grid. Because of the interactions between the alkyl chains covered on the surfaces, parts of them self-assemble into parallel superstructures, the distances between which can be estimated to be about 3−4 nm, corresponding to the double length of the surface layers of the coatings. HRTEM analysis shows direct evidence that these structures are indeed nanotubes. As shown in Figure 1b,c, the HAp nanotubes show apparent hollow structures, and the wall thickness is estimated to be about ~3 nm. The characterization over the wall shows that it is well-crystalline, and the lattice spacing can be calculated to be ~0.347 nm, corresponding to the (002) planes of HAp (Figure 1f). Energy-dispersive spectrometry (EDS) patterns taken from single nanotubes show that they are indeed single crystals (Figure 1e,i, inset). EDS taken from single nanotubes shows the existence of F, Ca, P, and O in the final products (SFig. 1 in the Supporting Information). The ratio between P and Ca is calculated to be ~1.54, within the generally accepted range between 1.5 and 1.67, and the ratio between F and Ca is calculated to be ~0.035, indicating the successful incorporation of F into HAp.

It is worth noting that with an increase of the F^- to Ca ratio from 0.033 to 0.25, the aspect ratios of the HAp nanotubes will decrease, and the diameters will increase from 10 to 20 nm while the lengths will decrease from 200 to 50 nm (Figure 1j). The difference in the aspect ratio of the HAp nanotubes can satisfy the demands for potential applications in artificial bones and teeth. HRTEM characterization over the HAp nanotubes with higher F^- doping levels shows that they are quite different from those with lower F^- doping levels. As shown in Figure 1h,i, large nanopores distribute evenly along the nanotube while the walls around the pores are well-crystallined with thicknesses of around 2 nm.

Powder X-ray diffraction (XRD) patterns (SFig. 3 in the Supporting Information) taken from these nanotubes show that they can be indexed as the hexagonal phase of $Ca_{10}(PO_4)_6(OH)_2$ (space geoup *P*63/*m*[176]) with lattice constants $a = 0.942$ nm and $c = 0.688$ nm (JCPDS 74-0566). With an increase in the doping level of F^-, all of the peaks shift to higher degrees, indicating shrinkage of the lattice volume in HAp. The shrinkage was apparently induced by the replacement of −OH by F^-. IR spectra were taken from the HAp nanotubes with different levels of F substitution, from which absorption bands of $-CH_3$, $-CH_2$, P−O, and −COOH groups can be clearly observed. The intensities of the absorption peak corresponding to −OH dramatically decrease with an increase in the doping levels of F into HAp, while the intensities of other peaks remain almost the same, indicating the successful replacement of −OH by F^-. It can also be observed that the intensities for $x = 0.167$ and 0.100 differ marginally, whereas the intensities for $x = 0.033$ and 0.100 differ significantly. On the basis of this phenomena, it is most probable that the replacement of −OH by F^- mainly occurred inside the nanotubes in the case of 3% doping while the −OH groups on the outside surface could also be replaced with increases of 3% to 10% and 16.7%.

Control experiments were carried out to investigate the formation mechanism of these nanotubes. It was found that the addition order of F^- and PO_4^{3-} played an important role in the formation process of these nanotubes. When F^- was added to the system before PO_4^{3-}, uniform nanotubes could be obtained in a wide F^- concentration range from 0.033 to 0.25. However, when PO_4^{3-} was added before F^-, only nanorods with small pores on the surfaces could be obtained. These experiments proved that the formation of nanotubes was closely related to the addition order of the reagents. XRD patterns were taken from the products obtained after stirring at room temperature without hydrothermal treatment, and it was clear that CaF_2 formed at first in the system (SFig. 4 in the Supporting Information). TEM images taken from the colloidal mixture showed that they were composed of irregular amorphous particles. Then after hydrothermal treatment for about 1 h, the HAp phase appeared and CaF_2 vanished, which indicated that along with the growth process CaF_2 would react with the absorbed PO_4^{3-} to form HAp with F^- doped into the lattice. TEM images taken from the 1 h samples show that they are composed of uniform nanorods with sharp tips (Figure 2a). HRTEM characterization clearly shows the distribution of small pores inside the nanorods (Figure 2b). Considering that HAp has anistropic hexagonal structure in nature, it is reasonable to imagine that HAp coated on the surface of CaF_2 could guide the growth of the CaF_2@HAp structures, which may lead to the formation of 1-D nanostructures and not hollow spheres. With the complete transformation of CaF_2 into F-substituted HAp, CaF_2 was totally consumed and a hollow interior space

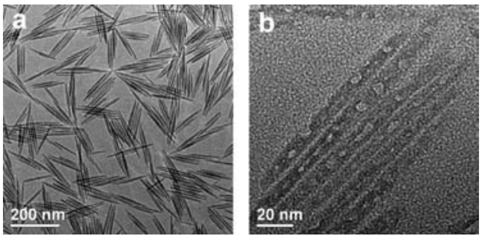

Figure 2. (a) Representative TEM image of F-HAp nanorods with sharp tips taken from samples after 1 h of reaction (F/Ca = 0.033, 100 °C). (b) HRTEM images of F-HAp nanorods with sharp tips showing the small pores inside the nanorods.

was left with the formation of nanotubes. On the basis of these experimental results, it is believed that the diffusion-controlled Kirkendall effect[19] plays an important role in this process. The relatively high reactivity of the in situ generated CaF_2 is important for the success of this approach. This mechanism can also explain the formation of porous structures and the decrease in the aspect ratios with higher doping levels of F^- in that more aggregated CaF_2 amorphous particles can leave some larger holes on the nanorods and break their anisotropic growth to some extent.

At a lower temperature range of 90−150 °C, these nanotubes usually have hydrophobic surface properties and can be dispersed into nonpolar solvents like cyclohexane and chloroform (Figure 3a), while those obtained at a higher temperature range of 200−220 °C have hydrophilic properties and can be dispersed into polar solvents like water and ethanol (Figure 3b). In a similar way, the aspect ratio of the nanotubes can be tuned with the doping level of F^-. The change in the surface properties may be attributed to the differences in the monolayer or bilayer absorption modes of long-alkyl-chain surfactants on the nanotubes. With an increase in the temperature, it is most probable that the long-alkyl-chain surfactants would absorb onto the surface of the F-HAp nanotubes in the form of double layers, which would leave the hydrophilic groups outside.[8,20]

While effective in tuning the surface properties of the nanotubes by controlling the temperatures, this method can only generate hydrophilic or hydrophobic nanotubes in one pot (Figure 3a,b). We find that the addition of PEG into the reaction system will generate nanotubes with universal dispersibility in solvents, including water, ethanol, cyclohexane, and chloroform (Figure 3c). The as-obtained colloidal solution can remain stable, and no apparent precipitants can be observed. As shown in Figure 3d, the F-HAp nanostructures dispersed in either water or cyclohexane are all uniform nanotubes. A magnified TEM image (Figure 3e) further reveals their interior hollow structures. On the basis of our studies and previous investigations, it is proposed that the amphiphilic surface properties of these F-HAp nanotubes can be attributed to the coanchoring of the amphiphilic multidentate ligand PEG (MW 20 000) and hydrophobic oleic acid on the outer surface of the nanotubes. IR spectra taken from the amphiphilic nanotubes clearly show the coexistence of −OH and alkyl chains (SFig. 5b in the Supporting Information). It was found that the molecular weight of PEG had a great influence on the surface properties of the nanotubes. Only PEG with MW higher than 10 000 can ensure the amphiphilic surface properties of the nanotubes.

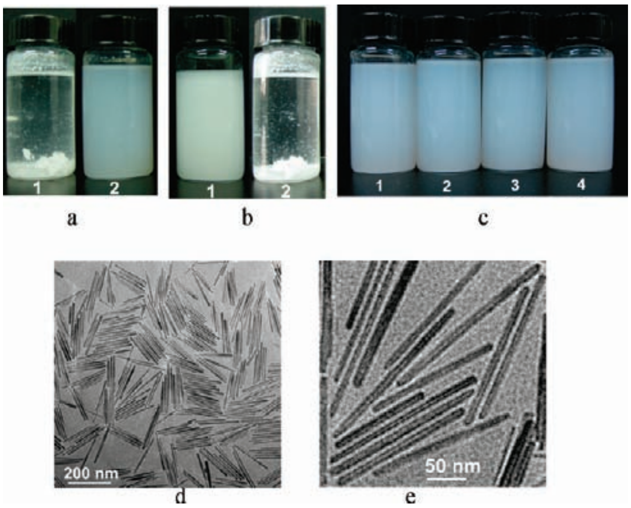

Figure 3. (a) Solubility of the F-HAp nantubes with hydrophobic surface properties (4 mL of oleic acid and 0.5 g of octadecylamine, 100 °C) in water (1) and cyclohexane (2). The weight ratio between the nanotubes and solvents is kept at 3−5%. (b) Solubility of the F-HAp nantubes with hydrophilic surface properties (4 mL of oleic acid and 0.5 g of octadecylamine, 220 °C) in water (1) and cyclohexane (2). The weight ratio between the nanotubes and solvents is kept at 3−5%. (c) Solubility of the F-HAp nantubes with amphiphilic surface properties [0.5 g of PEG (MW = 20 000) and 4 mL of oleic acid, 100 °C] in water (1), ethanol (2), cyclohexane (3), and chloroform (4). The weight ratio between the nanotubes and solvents is kept at 3−5%. (d) TEM images of the amphiphilic F-HAp nanotubes. (e) Magnified TEM images showing the structures of hollow nanotubes.

In this Communication, monodisperse F-substituted HAp nanotubes with different aspect ratios and amphiphilic surface properties have been successfully prepared via a hydrothermal synthetic route. A small amount of ~3% F doping in HAp can lead to the formation of nanotubes. This study will provide not only novel building blocks for the construction of artificial bones with novel mechanical properties but also a new strategy for the controlled growth of inorganic nanotubes.

Acknowledgment. This work was supported by NSFC (Grant 20725102), the Foundation for the Author of National Excellent Doctoral Dissertation of People's Republic of China, the Program for New Century Excellent Talents of the Chinese Ministry of Education, the Fok Ying Tung Education Foundation (Grant 111012), and the State Key Project of Fundamental Research for Nanoscience and Nanotechnology (Grant 2006CB932301).

Supporting Information Available: XRD patterns of F-HAp nanotubes with different doping levels and at different reaction stages, EDS analysis spectra of F-HAp nanotubes, and IR spectra of F-HAp nanotubes with hydrophilic surface properties (220 °C) and amphiphilic surface properties (100 °C). This material is available free of charge via the Internet at http://pubs.acs.org.

---

(19) Liang, X.; Wang, X.; Zhuang, Y.; Xu, B.; Kuang, S. M.; Li, Y. D. *J. Am. Chem. Soc.* **2008**, *130*, 2736–2737.

(20) Pellegrino, T.; Manna, L.; Kudera, S.; Liedl, T.; Koktysh, D.; Rogach, A. L.; Keller, S.; Radler, J.; Natile, G.; Parak, W. L. *Nano Lett.* **2004**, *4*, 703.